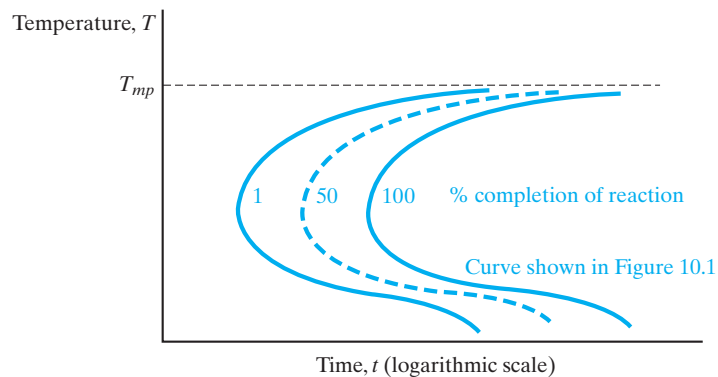


---

## 10.2 The TTT Diagram

---

The preceding section introduced time as an axis in monitoring microstructural development. The general term for a plot of the type shown in Figure 10.1 is a **TTT diagram**, where the letters stand for temperature, time, and (percent) transformation. This plot is also known as an **isothermal transformation diagram**. In the case of Figure 10.1, the time necessary for 100% completion of transformation was plotted. Figure 10.6 shows how the progress of the transformation can be traced with a family of curves showing different percentages of completion. Using the industrially important eutectoid transformation in steels as an example, we can now discuss in further detail the nature of **diffusional transformations** in solids (a change in structure due to the long-range migration of atoms). In addition, we shall find that some **diffusionless transformations** play an important role in microstructural development and can be superimposed on the TTT diagrams.



**FIGURE 10.6** A time–temperature–transformation diagram for the solidification reaction of Figure 10.1 with various percent completion curves illustrated.

## DIFFUSIONAL TRANSFORMATIONS

Diffusional transformations involve a change of structure due to the long-range migration of atoms. The development of microstructure during the slow cooling of eutectoid steel (Fe with 0.77 wt % C) was shown in Figure 9.38. A TTT diagram for this composition is shown in Figure 10.7. It is quite similar to the schematic for solidification shown in Figure 10.1. The most important new information provided in Figure 10.7 is that **pearlite** is not the only microstructure that can develop from the cooling of **austenite**. In fact, various types of pearlite are noted at various transformation temperatures. The slow cooling path assumed in Chapter 9 is illustrated in Figure 10.8 and clearly leads to the development of a coarse pearlite. Here, all references to size are relative. In Chapter 9, we made an issue of the fact that eutectic and eutectoid structures are generally fine grained. Figure 10.7 indicates that the pearlite produced near the eutectoid temperature is not as fine grained as that produced at slightly lower temperatures. The reason for this trend can be appreciated by studying Figure 10.5. Low nucleation rates and high diffusion rates near the eutectoid temperature lead to a relatively coarse structure. The increasingly fine pearlite formed at lower temperatures is eventually beyond the resolution of optical microscopes (approximately  $0.25\ \mu\text{m}$  features observable at about  $2,000\times$  magnification). Such fine structure can be observed with electron microscopy because electrons have effective wavelengths much smaller than those in the visible light range.

Pearlite formation is found from the eutectoid temperature ( $727^\circ\text{C}$ ) down to about  $400^\circ\text{C}$ . Below  $400^\circ\text{C}$ , the pearlite microstructure is no longer formed. The ferrite and carbide form as extremely fine needles in a microstructure known as **bainite**\* (Figure 10.9), which represents an even finer distribution of ferrite and carbide than in fine pearlite. Although a different morphology is found in bainite, the general trend of finer structure with decreasing temperature is continued. It is important to note that the variety of morphologies that develops over the range of temperatures shown in Figure 10.7 all represent the same phase

\*Edgar Collins Bain (1891–1971), American metallurgist, discovered the microstructure that now bears his name. His many achievements in the study of steels made him one of the most honored metallurgists of his generation.

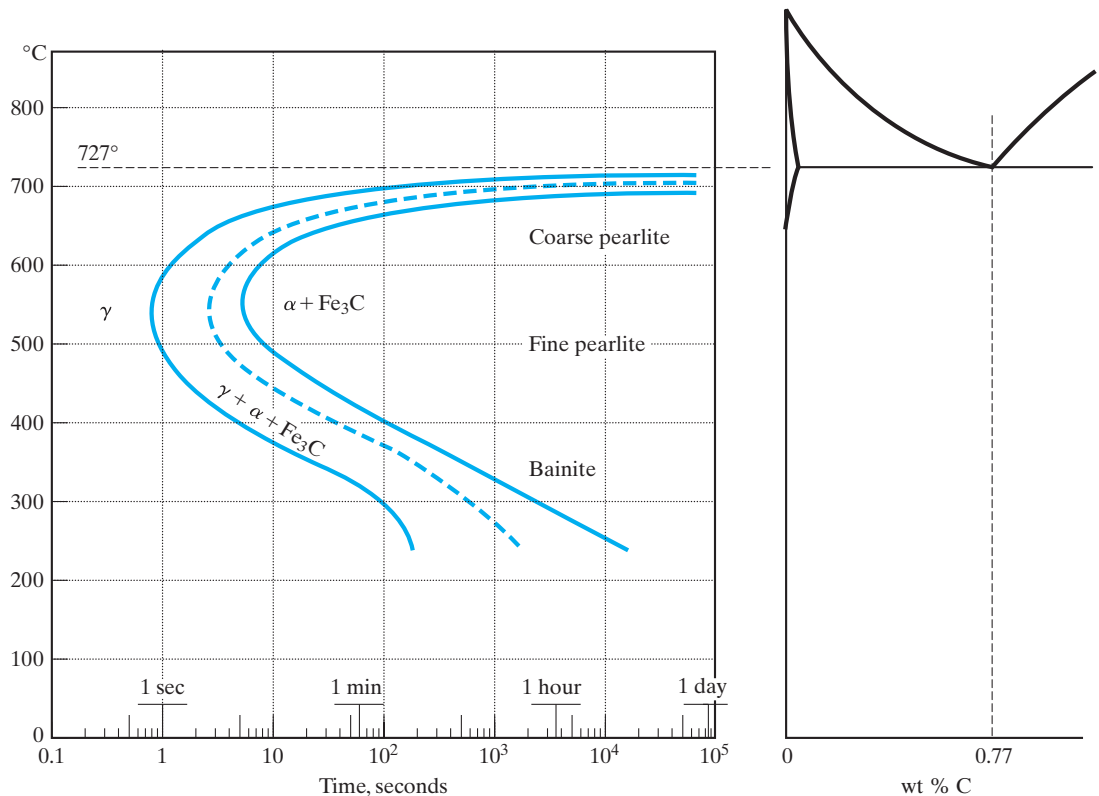


**FIGURE 10.7** TTT diagram for eutectoid steel shown in relation to the Fe–Fe<sub>3</sub>C phase diagram (see Figure 9.38). This diagram shows that, for certain transformation temperatures, bainite rather than pearlite is formed. In general, the transformed microstructure is increasingly fine grained as the transformation temperature is decreased. Nucleation rate increases and diffusivity decreases as temperature decreases. The solid curve on the left represents the onset of transformation (~1% completion). The dashed curve represents 50% completion. The solid curve on the right represents the effective (~99%) completion of transformation. This convention is used in subsequent TTT diagrams. (TTT diagrams after Atlas of Isothermal Transformation and Cooling Transformation Diagrams, American Society for Metals, Metals Park, OH, 1977)

compositions and relative amounts of each phase. These terms all derive from the equilibrium calculations (using the tie line and lever rule) of Chapter 9. It is equally important to note that TTT diagrams represent specific thermal histories and are not state diagrams in the way that phase diagrams are. For instance, coarse pearlite is more stable than fine pearlite or bainite because it has less total interfacial boundary area (a more disordered region as discussed in Section 4.4 and thereby a higher energy region). As a result, coarse pearlite, once formed, remains upon cooling, as illustrated in Figure 10.10.

### DIFFUSIONLESS (MARTENSITIC) TRANSFORMATIONS

The eutectoid reactions in Figure 10.7 are all diffusional in nature. But close inspection of that TTT diagram indicates that no information is given below about 250°C. Figure 10.11 shows that a very different process occurs at lower

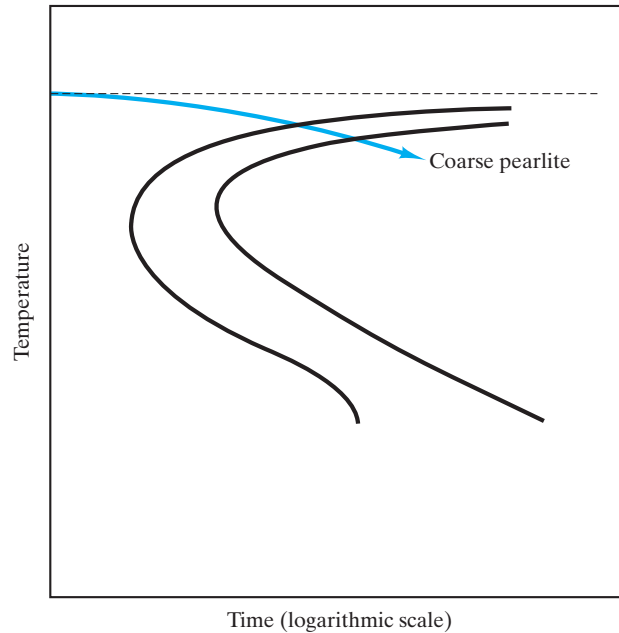


**FIGURE 10.8** A slow cooling path that leads to coarse pearlite formation is superimposed on the TTT diagram for eutectoid steel. This type of thermal history was assumed, in general, throughout Chapter 9.

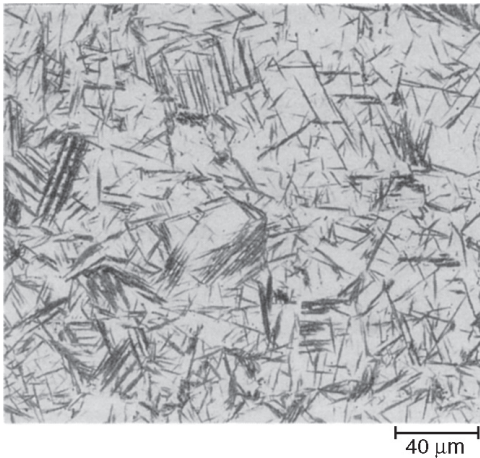


**FIGURE 10.9** The microstructure of bainite involves extremely fine needles of ferrite and carbide, in contrast to the lamellar structure of pearlite (see Figure 9.2), 250 $\times$ . (From ASM Handbook, Vol. 9, Metallography and Microstructures, ASM International, Materials Park, OH, 2004.)

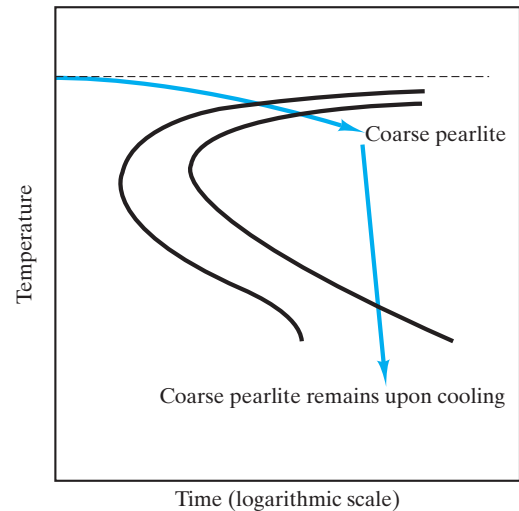


**FIGURE 10.10** The interpretation of TTT diagrams requires consideration of the thermal history “path.” For example, coarse pearlite, once formed, remains stable upon cooling. The finer-grain structures are less stable because of the energy associated with the grain-boundary area. (By contrast, phase diagrams represent equilibrium and identify stable phases independent of the path used to reach a given state point.)

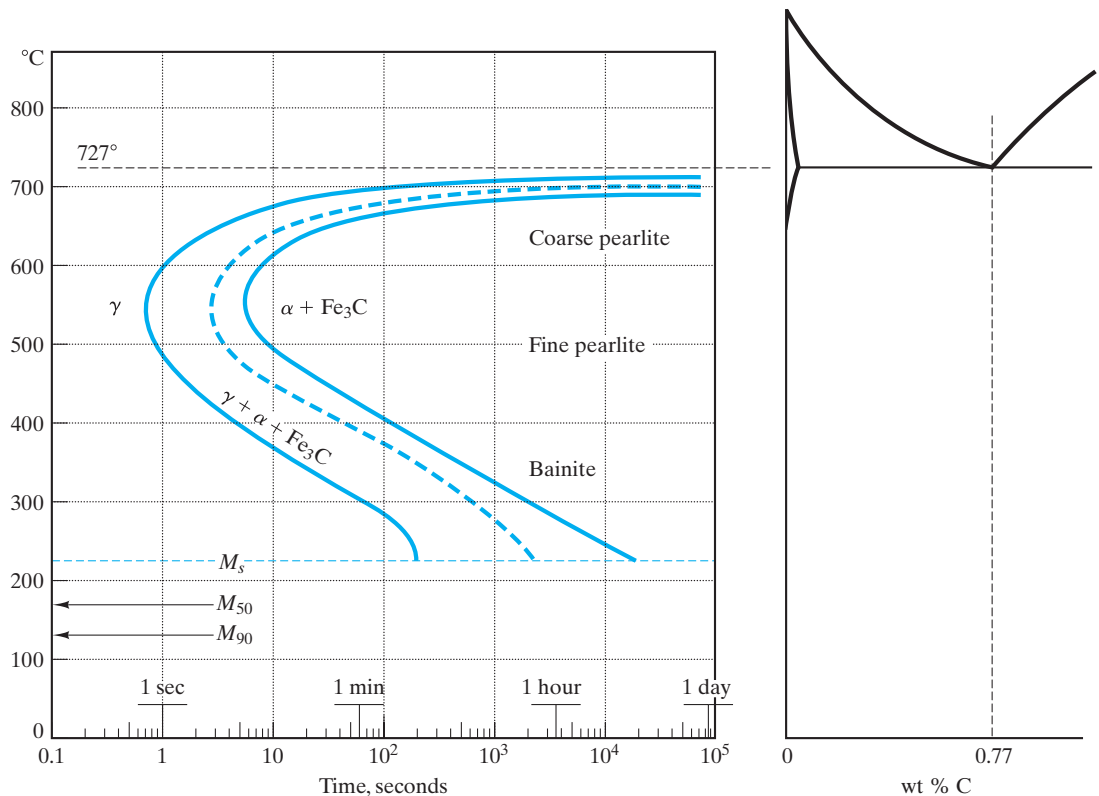


**FIGURE 10.11** A more complete TTT diagram for eutectoid steel than was given in Figure 10.7. The various stages of the time-independent (or diffusionless) martensitic transformation are shown as horizontal lines.  $M_s$  represents the start,  $M_{50}$  represents 50% transformation, and  $M_{90}$  represents 90% transformation. One hundred percent transformation to martensite is not complete until a final temperature ( $M_f$ ) of  $-46^\circ\text{C}$ .

temperatures. Two horizontal lines are added to represent the occurrence of a *diffusionless* process known as the **martensitic\* transformation**. This generic term refers to a broad family of diffusionless transformations in metals and nonmetals alike. The most common example is the specific transformation in eutectoid steels. In this system, the product formed from the quenched austenite is termed **martensite**. In effect, the quenching of austenite rapidly enough to bypass the pearlite “knee” at approximately  $550^\circ\text{C}$  allows any diffusional transformation to be suppressed. However, there is a price to pay for avoiding the diffusional process. The austenite phase is still unstable and is, in fact, increasingly unstable with decreasing temperature. At approximately  $215^\circ\text{C}$ , the instability of austenite is so great that a small fraction (less than 1%) of the material transforms spontaneously to martensite. Instead of the diffusional migration of carbon atoms to

\*Adolf Martens (1850–1914), German metallurgist, was originally trained as a mechanical engineer. Early in his career, he became involved in the developing field of testing materials for construction. He was a pioneer in using the microscope as a practical analytical tool for metals. Later, in an academic post, he produced the highly regarded *Handbuch der Materialienkunde* (1899).

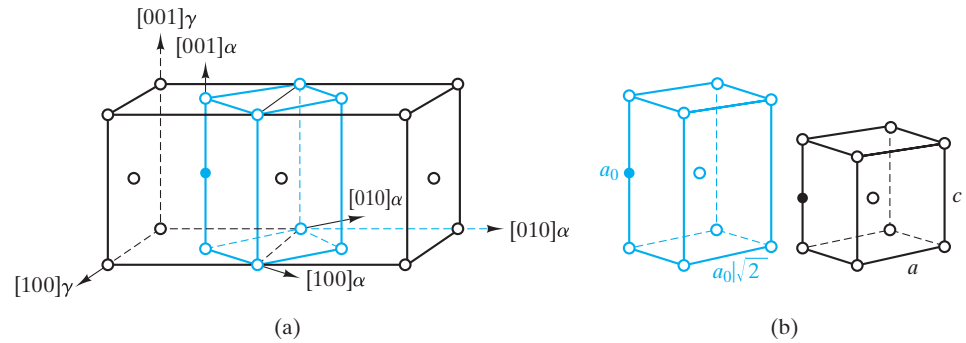


**FIGURE 10.12** For steels, the martensitic transformation involves the sudden reorientation of C and Fe atoms from the fcc solid solution of  $\gamma$ -Fe (austenite) to a body-centered tetragonal (bct) solid solution (martensite). In (a), the bct unit cell is shown relative to the fcc lattice by the  $\langle 100 \rangle_\alpha$  axes. In (b), the bct unit cell is shown before (left) and after (right) the transformation. The open circles represent iron atoms. The solid circle represents an interstitially dissolved carbon atom. This illustration of the martensitic transformation was first presented by Bain in 1924, and while subsequent study has refined the details of the transformation mechanism, this diagram remains a useful and popular schematic. (After J. W. Christian, in *Principles of Heat Treatment of Steel*, G. Krauss, Ed., American Society for Metals, Metals Park, OH, 1980.)

produce separate  $\alpha$  and  $\text{Fe}_3\text{C}$  phases, the martensite transformation involves the sudden reorientation of C and Fe atoms from the face-centered cubic (fcc) solid solution of  $\gamma$ -Fe to a body-centered tetragonal (bct) solid solution, which is martensite (Figure 10.12). The relatively complex crystal structure and the supersaturated concentration of carbon atoms in the martensite lead to a characteristically brittle nature. The start of the martensitic transformation is labeled  $M_s$  and is shown as a horizontal line (i.e., time independent) in Figure 10.11. If the quench of austenite proceeds below  $M_s$ , the austenite phase is increasingly unstable, and a larger fraction of the system is transformed to martensite. Various stages of the martensitic transformation are noted in Figure 10.11. Quenching to  $-46^\circ\text{C}$  or below leads to the complete transformation to martensite. The acicular, or needlelike, microstructure of martensite is shown in Figure 10.13. Martensite is a **metastable** phase; that is, it is stable with time, but upon reheating it will decompose into the even more stable phases of  $\alpha$  and  $\text{Fe}_3\text{C}$ . The careful control of the proportions of these various phases is the subject of heat treatment, which is discussed in the next section.

As one might expect, the complex set of factors (discussed in Section 10.1) that determine transformation rates requires the TTT diagram to be defined in terms of a specific thermal history. The TTT diagrams in this chapter are generally *isothermal*; that is, the transformation time at a given temperature represents the time for transformation at the fixed temperature following an instantaneous quench. Figure 10.8 and several subsequent diagrams will superimpose cooling or heating paths on these diagrams. Such paths can affect the time at which the transformation will have occurred at a given temperature. In other words, the positions of transformation curves are shifted slightly downward and toward the right for nonisothermal conditions. Such a **continuous cooling transformation (CCT) diagram** is shown in Figure 10.14. For the purpose of illustration, we shall not generally make this refinement in this book. The principles demonstrated are, nonetheless, valid.

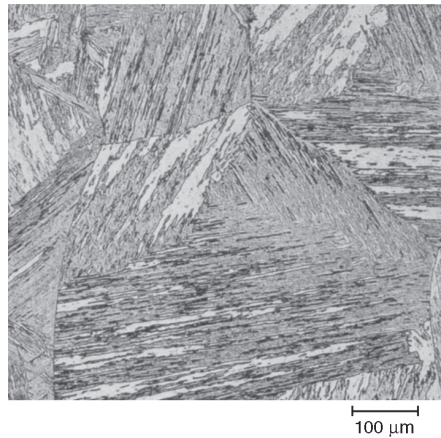


**FIGURE 10.13** Acicular, or needlelike, microstructure of martensite 100 $\times$ . (From ASM Handbook, Vol. 9, Metallography and Microstructures, ASM International, Materials Park, OH, 2004.)

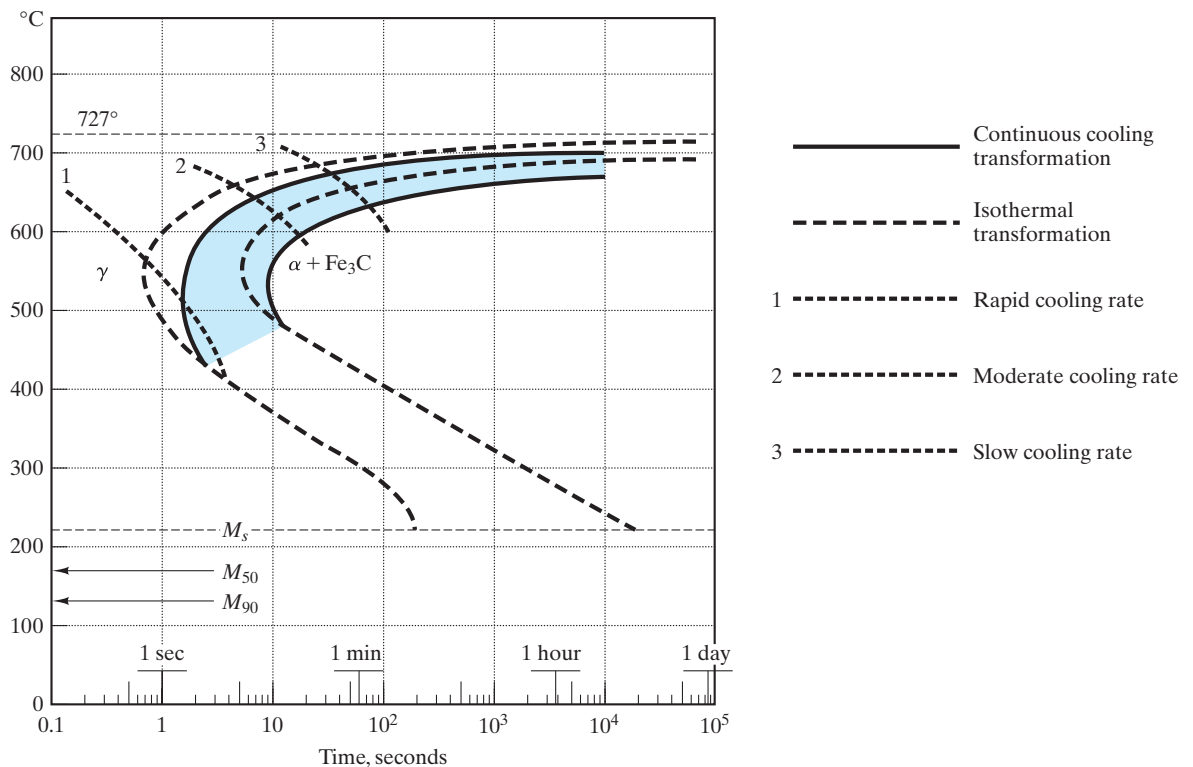


**FIGURE 10.14** A continuous cooling transformation (CCT) diagram is shown superimposed on the isothermal transformation diagram of Figure 10.11. The general effect of continuous cooling is to shift the transformation curves downward and toward the right. (After Atlas of Isothermal Transformation and Cooling Transformation Diagrams, American Society for Metals, Metals Park, OH, 1977)

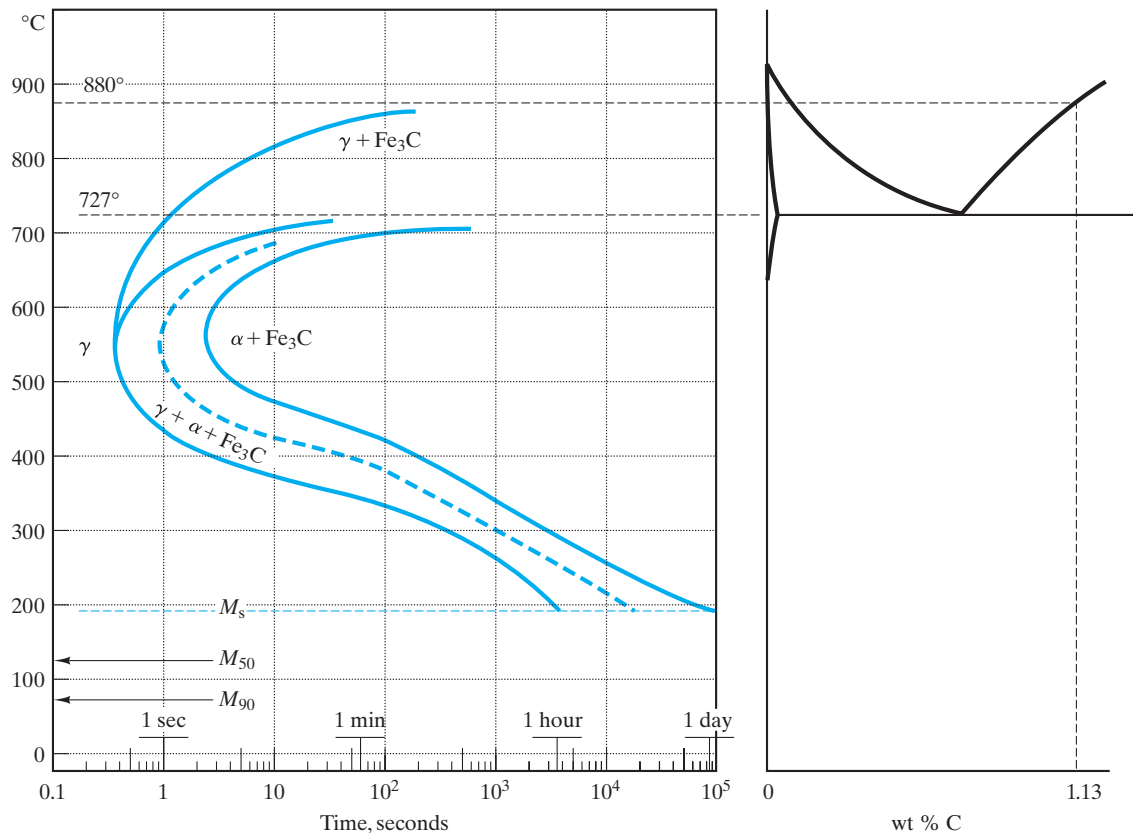


**FIGURE 10.15** TTT diagram for a hypereutectoid composition (1.13 wt % C) compared with the Fe–Fe<sub>3</sub>C phase diagram. Microstructural development for the slow cooling of this alloy was shown in Figure 9.39. (TTT diagram after Atlas of Isothermal Transformation and Cooling Transformation Diagrams, American Society for Metals, Metals Park, OH, 1977.)

Our discussion to this point has centered on the eutectoid composition. Figure 10.15 shows the TTT diagram for the hypereutectoid composition introduced in Figure 9.39. The most obvious difference between this diagram and the eutectoid is the additional curved line extending from the pearlite “knee” to the horizontal line at 880°C. This additional line corresponds to the additional diffusional process for the formation of proeutectoid cementite. Less obvious is the downward shift in the martensitic reaction temperatures, such as  $M_s$ . A similar TTT diagram is shown in Figure 10.16 for the hypoeutectoid composition introduced in Figure 9.40. This diagram includes the formation of proeutectoid ferrite and shows martensitic temperatures higher than those for the eutectoid steel. In general, the martensitic reaction occurs at decreasing temperatures with increasing carbon contents around the eutectoid composition region.